An Experimental Investigation on Axial Heat Flux of Wall in Microtubes

Duan Zhen[1], Zhao Xiaobao[2], Liu Zhigang[3]

(1. Nanjing Institute of Boiler & Pressure Vessel Supervisory Inspection, Nanjing 210002, China;
2. School of Power Engineering, Nanjing Normal University, Nanjing 210042, China;
3. Shandong Energy Research Institute Academy of Sciences, Jinan 250014, China)

Abstract: This paper investigates the characteristics of wall temperature field and axial wall heat conduction of stainless steel microtubes with inner diameters of 168 m and 399 m, as distilled water flows through the stainless steel microtube. Based on thermal imaging technology of micro area, the temperature distribution maps on the wall of microtubes are obtained by employing an IR Camera for constant Reynolds number and different heating powers. A simple mathematic model is used to express the relationship between the axial wall conductive heat and the fluid convective heat transfer. The experimental results and theoretical analysis show that the quantity of axial wall conductive heat is considerably small and may be neglected compared to the convective heat transfer for liquid flow in microtube.

Key words: micro heat transfer; microtube; micro flow; IR camera

CLC number: TK124, **Document code**: A, **Article ID**: 1672-1292(2008)01-0038-09

微管道内壁面轴向热流实验研究

端 震[1], 赵孝保[2], 刘志刚[3]

(1. 南京市锅炉压力容器检验所, 江苏 南京 210002; 2. 南京师范大学 动力工程学院, 江苏 南京 210042;
3. 山东省科学院 能源研究所, 山东 济南 250014)

[摘要] 以蒸馏水流过内径分别为 168 m和 399 m的不锈钢微管, 研究了微管壁面温度分布和壁面轴向导热特征. 依据微面热成像技术, 用红外热像仪获得了恒定雷诺数和不同加热功率下微管壁面温度分布图. 用一个简化的数学模型表示了壁面轴向导热和流体对流传热关系. 实验和理论分析表明微管内壁面轴向导热量微小, 与液体对流换热相比可以忽略.

[关键词] 微传热、微管, 微流动, 红外热像仪

With the rapid development in bioengineering and biotechnology, aerospace, microelectronics, materials processing and manufacturing etc, more and more researchers are engaged in the study about the microscale flow and heat transfer. In the earliest investigation of microscale flow and heat transfer, Tuckermann and Pease[1] studied the fluid flow and heat transfer characteristics in microchannels, and demonstrated that electronic chips could be effectively cooled by means of the forced convective flow of water through microchannels fabricated either directly in the silicon wafer or in the circuit board on which the chips were mounted. Wu and Little[2] measured the heat transfer characteristics for gas flow in miniature channels with inner diameter ranging from 134 to 164 m. The tests involved both laminar and turbulent flow regimes. Their results showed that the turbulent convention occurs at a Reynolds number of approximately 1 000. They also found that the convective hear transfer characteristics depart from the predictions of the established empirical correlations for macroscale tubes. They attributed these deviations to the asymmetric roughness and the large relative roughness of the microchannel walls; Choi et al[3] measured the convective heat transfer coefficient for the flow of nitrogen gas in microtubes with inner diameter ranging from 3 to 81 m for both laminar and turbulent regimes. In contrast to the conventional predic-

Received date: 2007-08-20.
Foundation item: Supported by the Natural Science Foundation of Jiangsu Province (Grant No. BK2006222).
Biography: Duan Zhen (1975-), Engineer, field of study: special type equipment inspection, management and research. E-mail: dz9322@sina.com

tion, they found that the measured Nusselt number exhibits a Reynolds number dependence in full-developed laminar flow and the measured Nusselt numbers are larger than those predicted by the Dittus-Boelter correlation and the Colburn analogy is no longer valid in turbulent flow. No early transition to turbulent convection was observed. Wang and Peng[4] also experimentally studied the forced flow convection of liquid in microchannels and found that the fully developed turbulent convection was initiated at Reynolds numbers in the range of 1 000~1 500, and that the conversion from the laminar to transition region occurred in the range of 300~800. The heat transfer behavior in the laminar and transition regions was found to be quite unusual and complicated. Peng and Peterson[5] later confirmed these experimental observations using methanol flowing through similar microchannel structures and analyzed experimentally the effects of the thermofluid and the geometric variables on the heat transfer. Yu et al[6] studied the convective heat transfer characteristics of water in microtubes with diameters of 19, 52, and 102 μm. The experiments were performed for turbulent regimes with Reynolds number greater than 2 500. It was found that at a low Reynolds number, the heat transfer data from microtubes and large tubes were more or less the same, but the values diverge as the Reynolds number increased. Values of the Nusselt number were always higher than those predicted by the conventional correlations. The Colburn factor changes with the Reynolds number. Adams et al[7] experimentally investigated the turbulent convective heat transfer of water in microtubes with inner diameters of 760 and 1 090 μm. Their results showed that Nusselt number for the microtubes is higher than that predicted by the conventional empirical correlations for macroscale tubes.

In the above cited literatures, there is considerable disagreement about the effects of microscale on the flow and heat transfer. Most of studies showed that the Nusselt number for microscale heat transfer is higher than those traditional correlations for macroscale. Some researchers[8] attributed this enhancement to thinning of the boundary layer in the narrow channels, others[9] considered that the increase of the Nusselt number resulted from the size effects of microscale, such as the flow compressibility effects, the effect of roughness, the variation of predominate forces, the effect of surface geometry, the effect of surface electrostatic charges and the effect of axial heat conduction in the wall of microchannel or microtube etc. Of the microscale effects, only the effect of axial heat conduction along the wall will drop the convective coefficient for microscale heat transfer[10]. In general, the axial heat conduction in the channel or tube wall of conventional size can be neglected because the wall thickness is usually very small compared to the channel or tube diameter. However, the wall thickness may be of the same order of magnitude as or even larger than, the channels or tubes diameter, which will affect the flow and heat transfer in the microchannels or microtubes.

Only a limited number of literatures published to investigate the surface temperature characteristics of microtube or microchannel. Convective heat transfer in microtube, axial heat conduction, radiant heat transfer and convective heat transfer in the outer wall of microtube and so on, will affect the surface temperature distribution of microtube. It is very difficult to obtain the local temperature distribution by a conventional measurement method, e.g., thermocouples. However, the local temperature distribution is very important for analyzing the mechanisms of flow and heat transfer in microscale spaces.

In this study, an experimental method of visualization by using an IR camera is developed to get the photos of surface temperature distribution of microtubes with inner diameters of 168 and 399 μm. A detailed description of the surface temperature field of microtube is presented and discussed. These results provide new, fundamental comprehension for surface temperature characteristics in microtube.

1 Experimental Setup and Procedure

The test facility illustrated in Fig. 1 mainly consists of a pressure supply system, a liquid pool, a test section, a data acquisition system and an IR camera (JEOL, JTG-7300) etc. The stable and exact pressure nitrogen is supplied by the pressure supply system, which is formed by a nitrogen bottle, a three-layer filter, a precise pressure regulating valve, an air storage reservoir and a quick-opening valve. The nitrogen bottle, which is

capable of pressure to 12MPa, maintained precisely a given pressure (less than 1 6MPa) by a precise pressure regulating valve. In order to avoid any particles in the nitrogen from entering and contaminating the working fluid, the three-filter, with the aperture of filtration film of 50 m, 25 m, 5 m in turn, were installed between the nitrogen bottle and the precise pressure regulating valve. The function of gas storage reservoir was to avoid gas fluctuation.

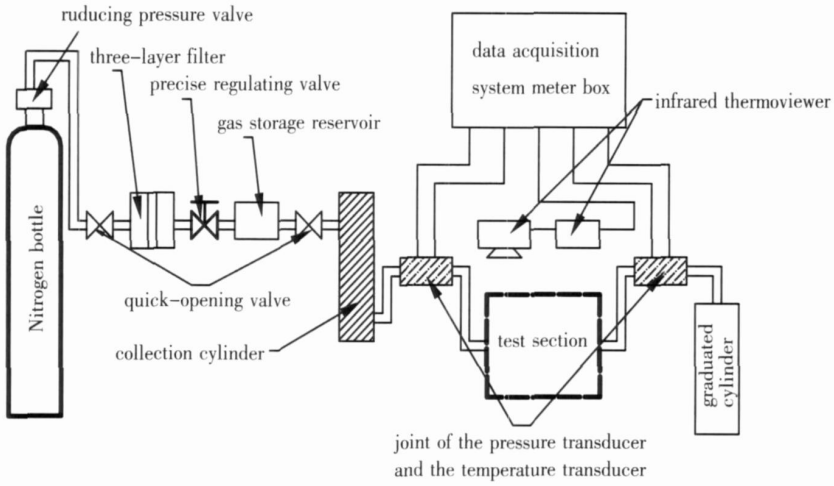

Fig.1 Schematic of the experimental test loop

Distilled water was used as the working fluid, which was deposited in the liquid pool. Water was pressed from the liquid pool by the high-pressure nitrogen and flowed through the test section. The liquid pool was connected by a small-diameter polyurethane tube with 2MPa resisting pressure to a joint just upstream of microtube. The cross-sectional area of polyurethane tube was over 50 times of that of the largest tested microtube, which assures that the fluid velocity in the polyurethane tube is negligibly small. Two calibrated pressure transducers, which were installed at the two-end joint of the test section, were used to measure the inlet and the outlet pressure of the microtube. The uncertainty in pressure measurement was 0 1% of the maximum reading. The transducers were adjusted before each test.

The fluid flow rate for a given pressure difference and a microtube sample was determined by collecting a liquid volume during a corresponding elapsed time. A high-precision graduated cylinder with an accuracy of 0 1 mL was used to measure the volume of the accumulated liquid. All of the tests were conducted with an increment of at least 5mL. The measurement was initiated after the prescribed experiment pressure was set by opening the reducing valve in the nitrogen bottle and adjusting the precise regulating valve, and the fluid flow became steady and the fluid level in the graduated cylinder reached a pre-set minimum. The elapsed time was then recorded while the level in the graduated cylinder reached a desired increment. The accuracy of the flow rate measurement was estimated to be 2%.

Precise liquid temperature measurements were necessary to determine the accurate values of the viscosity and the density. A K-type thermocouple with an accuracy of 0 1 was placed at the outlet of microtube to measure the exit temperature of the flow. Another thermocouple with the same type and accuracy was placed at the inlet to measure the entrance temperature of the flow, as shown in Fig 2. The thermocouples were calibrated before experiments. The measured temperatures were then used to determine the mean fluid temperature and to calculate the Nusslet number. The accuracy of the temperature measurement is estimated to be 0 3 .

Fig 2 gives a detailed view of the test section. An ampermeter and a voltmeter, whose accuracies are 0 02% and 0 01% of the maximum measurement range, respectively, were connected to the two-end of the test section and were used to measure the current and the voltage. In order to reduce the electrical contact resistance, sliver weld was used to join the red copper tube with the stainless steel microtube. The stainless steel microtube was electrically heated directly by a power source, which can supply low electric voltage and high electrical cur-

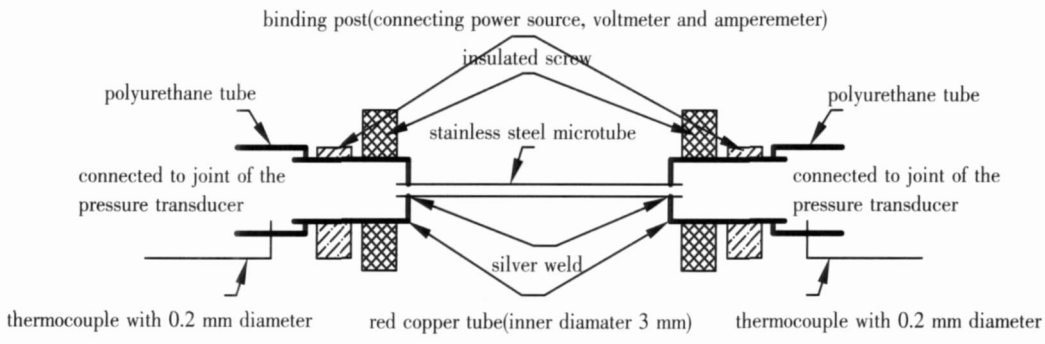

Fig.2 Schematic of the test section

rent. Thermal insulation material was attached to the exit section of microtube between the red copper tube and the measuring point of the thermocouple. The whole test section was installed in an optical bench, which can regulate precisely the distances in four directions of front, back, left and right.

A scanning electron microscope (SEM) was used to measure the inner diameter of the stainless steel microtube. Four scanning electron micrographs are shown in Fig. 3 and in Fig. 4. The microtube with the inner diameter of 399 μm featured smooth inner wall with few wall perturbations, while the wall of the microtube with the inner diameter of 168 μm was considerably rough. The four measurements of the inner diameter (two each at the microtube inlet and outlet) were averaged to minimize the measurement errors. The measurement results showed that the differences between average inlet and average outlet for stainless steel microtube were 2%. The uncertainty of the microtube diameter measurement mainly comes from the SEM systemic error at about 1%, the variation of multiplying power for measuring different microtubes and some artificial errors in the selection of tangent location, etc. The human bias is difficult to quantify and eliminate, and only increase the overall uncertainty in diameter measurement. However, the minimum uncertainty in diameter measurement for stainless steel microtube is estimated to be 5%[11].

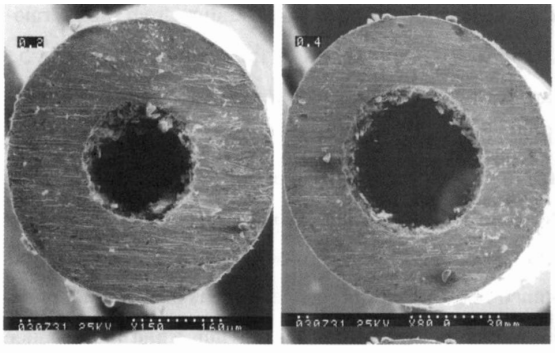

Fig.3 SEM image of the cross-section of a stainless steel microtube with inner diameter of 168 μm and 399 μm

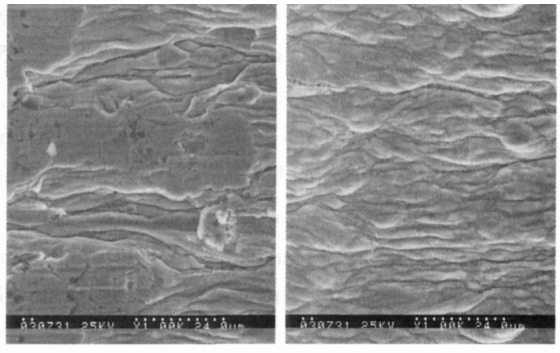

Fig.4 SEM image of the inner surface of a stainless steel microtube with inner diameter of 168 μm(left) and 399 μm(right)

The nitrogen gas in the nitrogen bottle acted as pressure source and drove the distilled water in the collection cylinder through the microtube. Diffusion of a small quantity of nitrogen gas into the working fluid is possible when the working fluid contacts with the pressed nitrogen in the collection cylinder. In addition, as the distilled water poured into the collection cylinder, it might absorb a little of air. Those might change heat transfer characteristics, especially in the microscale conditions. To reduce the uncertainty of gas absorption by distilled water, the purity of nitrogen gas in the nitrogen bottle reached 99.9% at least. Meanwhile, the distilled water was stored in an airtight container and was poured into the collection cylinder through a tube to avoid the air contact. The test showed that the gasification might be negligible for this study as the above-mentioned steps were taken. By the way, because the change of nitrogen gas pressure in the test is low (< 10 bar), the physical properties variations of the liquid are considered negligible.

Based on the microscale thermal-imaging technology, surface temperature distribution of the microtube was

measured by the high-precision IR camera, with a measuring range from 50 to 2000 and measuring accuracy 0 1 . The IR camera can confirm the surface temperature of an object according to the intensity of the surface infrared emissivity of the measured object.

Besides the temperature of the object, some other factors, such as the material and the surface conditions, also influence the surface emissivity of the object. Consequently, it is difficult to know the real emissivity of an object. There will be considerable temperature gaps between the real temperature and the measuring temperature gained by the IR camera if the real surface emissivity of the measured object is not known. Also, the distances between the thermoviewer lens and the measured object and the size of the measured object have great influences on the measured results. In addition, the light intensity in the environment also affects measurement results. In order to acquire real temperature distribution by the IR camera, many revising tests were conducted in the present study. We found that the temperatures at different points on the same object have the following relationship:

$$= \frac{T_1}{t_1} = \frac{T_2}{t_2} = \frac{T_3}{t_3} = \quad . \tag{1}$$

Where t_1, t_2, t_3 are the measured temperature values by the IR camera, T_1, T_2, T_3 are the real temperature values corresponding to t_1, t_2, t_3 respectively.

According to Eq. 1, only if a real temperature of a certain point in the temperature distribution picture taken by the IR camera was confirmed, could the real temperature field be acquired. Therefore, it is crucial to get the real temperature of a certain point in the temperature distribution picture. A K-type thermocouple with an accuracy of 0 1 was used to measure the temperature of the sliver weld that connects the stainless steel microtube and the red copper tube. It may be said that the real temperature of the section of the microtube was equal to that of the sliver weld, which is the measured temperature from the thermocouple. The photo from this test was illustrated in Fig. 5. The temperature values of the point N in the Fig. 5, which is the joint of the microtube and the thermocouple, are read by the thermocouple and by the IR camera respectively. The ratio of them is the value of g as shown in Eq. 1.

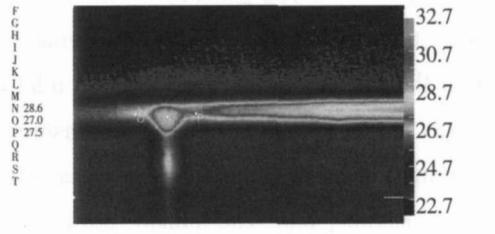

Fig.5 Temperature calibration photo for IR camera

Certainly, the distance between the lens of the IR camera and the microtube must be equal in whole tests, which requires that the horizontal errors from one end to the other end of the microtube sample must be less than 0 1mm. The length of the microtube taken by the IR camera each time depends on the distance between the lens of the IR camera and the microtube, and the larger the distance between the thermoviewer lens and the microtube is, the wider the IR camera could taken. The length in the microtube was taken about 21mm when the distance is 56mm. Compared to the shooting range of the IR camera, the diameter of the microtube is too thin, so a special magnifying lens, through which 99% of infrared ray can permeate, was used in the tests. The electric resistance of the red copper tube is different from that of the stainless steel microtube, especially at the joint of the lead wire and the red copper tube as well as the silver weld, thus, the heat produced by the electrical current is different too. The test showed that the heat produced at the joint was appreciably more than that at the other part of the microtube because of the bigger contact resistance of the red copper tube. Such a situation would appreciably affect the temperature distribution of the two-end of the microtube. In order to precisely measure the surface temperature field of the microtube, only the middle part of the microtube, which is about 10mm away from the two ends of the microtube sample, was photographed.

Swagelok fittings were used as the conduit connection of the experimental test loop to prevent leakage. The link tubes among the pressure supply system, the liquid pool, the test section and the graduated cylinder were the polyurethane tube with an inner diameter of 3 1 mm and 2MPa resisting pressure. All the measurement devices were connected to a computer data acquisition system. During a measurement, the pressure, as well as the

power source, was set to maintain a desired output. The pressure was regulated to produce a constant and needed flow rate. The output of the power source was set so as to obtain desired temperature distribution. For each measurement, the steady-state flow was considered when the readings of the temperatures did not change any more. At such a steady state, the temperature, the flow rate and the temperature field of the surface were monitored and recorded for about 20 min. The measurement for the same microtube was repeated at least thrice at the same flow rate and heating power. The uncertainties involved in the measurements are given in Table 1.

Table 1 Experimental uncertainties

Parameters	Uncertainties
Flow rate	2.0%
Current	0.02%
Voltage	0.01%
Diameter	5.3%
Temperature (IR Camera)	0.3

2 Results and Discussion

A number of experiments were conducted using stainless steel microtubes with the same tube length and different diameters. Photos taken by IR camera are presented in Figs. 6~7 for distilled water flow in the microtubes with inner diameters of 168 and 399 μm and outer diameter of 406 and 799 μm, respectively.

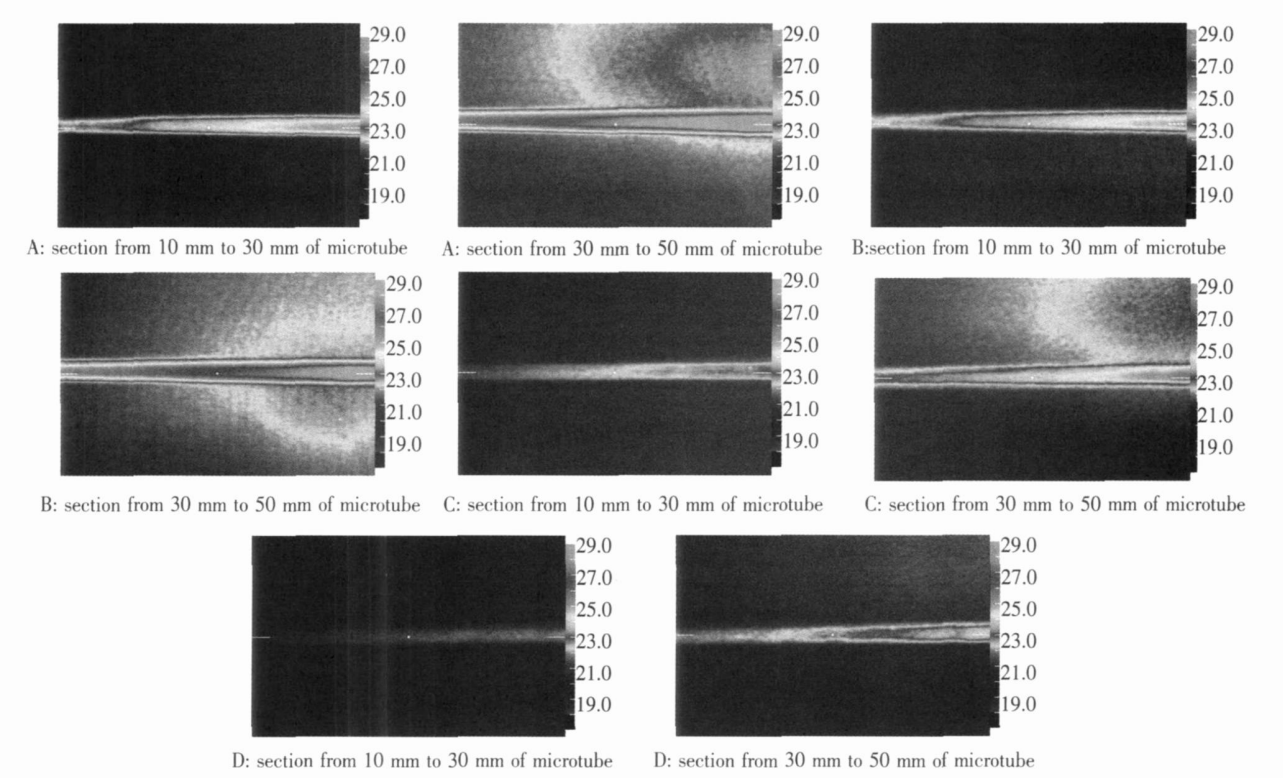

Fig.6 Axial surface temperature distribution photos on the microtube with inner diameter of 168 μm and outer diameter 406 μm, at Re=410 and heat flux of (A) 23.62 W/cm², (B) 19.04 W/cm², (C) 9.29 W/cm², (D) 5.58 W/cm²

In order to avoid the influence of light on taking, the all shots are conducted in the dark. The thermoviewer lens is only 56mm away from the surface of the microtube that can acquire better effect. However, the maximum length of the microtube is 21mm in each image at such a condition. Two shots must be made for the same microtube sample to obtain the surface temperature field of with 40mm length.

Figs. 6~7 show clearly the variation of surface temperature field with different heating power. By using the image processing software, the relative temperature values at any point, averaged temperature value on any area and the isotherm can be obtained. By equation (2), the modified temperature values can be obtained as shown in Fig. 8.

$$T = \quad T \qquad (2)$$

Where, T is modified temperature value. T is measuring value by IR camera. is correction factor and is

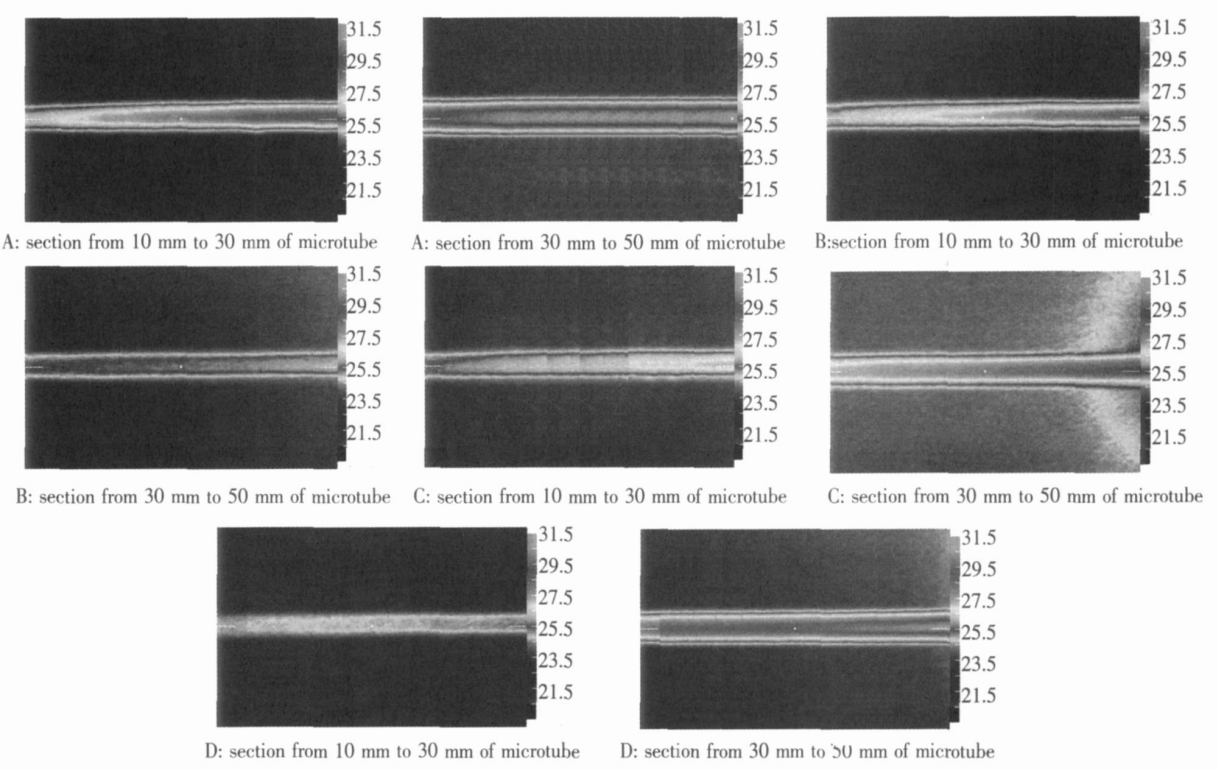

Fig.7　Axial surface temperature distribution photos on the microtube with inner diameter of 399 μm and outer diameter 799 μm, at Re=420 and heat flux of (A) 12.10 W/cm², (B) 9.79 W/cm², (C) 7.01 W/cm², (D) 3.63 W/cm²

defined as equation (1).

It is observed from Figs 6~ 8 that as heating power increases, the temperature gradient also increase. In the condition of same heating power, the temperature gradient is almost the same along with the entire wall of microtube. The average heat fluxes along the axis of the microtube for two different tube diameters are shown in Fig 8. Fig 8 indicates that axial heat flux with bigger ratio of the total cross-section area to the hole area of the microtube is greater.

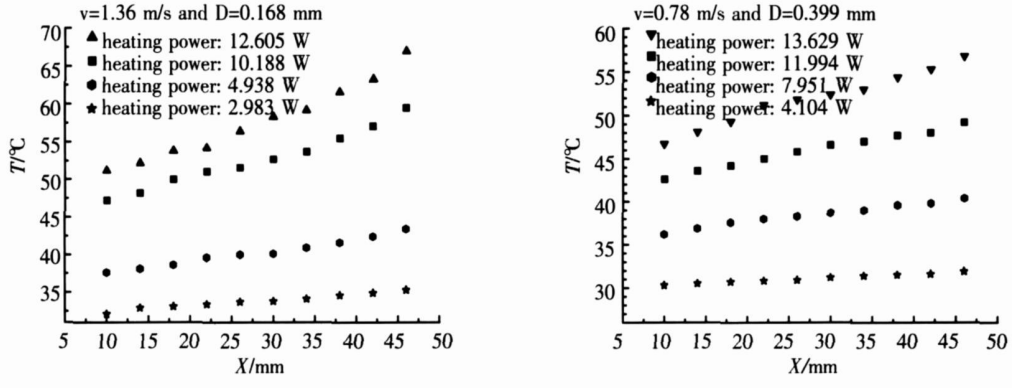

Fig.8　Surface temperature distribution on microtube wall

Because the inlet and outlet temperatures of the distilled water as well as the flow rate through the microtube were measured, the convection heat transfer in the microtube could be calculated and it is shown in Fig 9.

3　Theoretical Calculation About Influence of Axial Conduction on Convective Heat Transfer

The schematic of the theoretical calculation is shown in Fig 10.

Defining a differential control section X in the microtube, the ratio of axial wall conductive heat to convective heat can be represented as:

$$= \frac{Q_{con}}{Q_{cov}} = \frac{\frac{d}{dX}(q_{con} \quad (d+ \quad) \quad) \quad X}{q_{cov} \quad X \quad d} . \qquad (3)$$

Where, Q_{con} and Q_{cov} are the quantities of axial wall conduction along wall of the microtube and the convective heat transfer in the microtube, respectively, W; q_{con} and q_{cov} are the axial conductive heat flux along the wall and the convective heat flux in the microtube, respectively, W /m^2; d is the diameter of miotube, m; is the thickness of wall of the microtube, m.

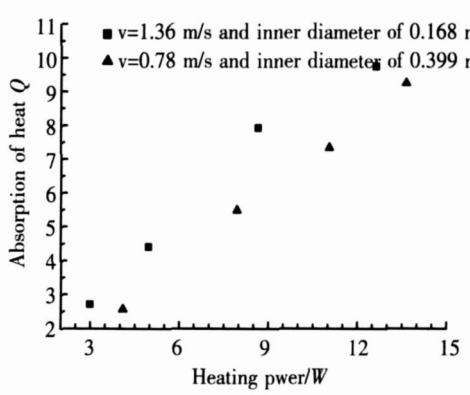

Fig.9 Relationship between convective heat and heating power

The axial wall heat conduction along wall of the microtube wall can be considered as one-dimensional and is expressed as:

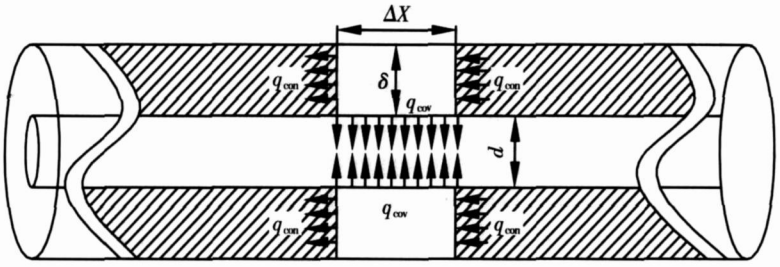

Fig.10 Schematic of analysis model

$$q_{con} = - k_s \frac{dT}{dX} ,$$

Thus:

$$= \frac{d}{q_{cov}\, dX}\left(- k_s \frac{dT}{dX}\right)\left(1+ \frac{}{d}\right) = - \frac{k_s}{q_{cov}} \frac{d^2T}{dX^2}\left(1+ \frac{}{d}\right) . \qquad (4)$$

Where, k_s is the thermal conductivity, is equal to 49 6W /(m K) for the stainless steel with 0 5% carbon.

According to Eq. 4, the effects of the axial wall conduction on the convective heat transfer are dominanted by the second order derivative of temperature in the axial direction, the wall thickness and the thermal conductivity of the microtube. Usually, it is very difficult to obtain $= \frac{^2T}{X^2}$ by a conventional measurement method. However, the surface temperature field of wall can be obtained by using the IR camera and thus the value of can be accurately gotten in the present study.

The curve in Fig. 8 is slight concave and thus the value of is plus. By fitting the temperature distribution functions temperature at different heating power and calculating the second derivative, the maximum value of is about 0 1K /m^2.

$$q_{cov} = \frac{Q}{F} . \qquad (5)$$

Where, Q is the quantity of convective heat transfer, W; F is the inner surface area, m^2.

Substituting the values of and q_{cov} into Eq. (4), the calculated value of is less than 0 1%, so the axial heat conduction along the wall can be neglected compared to the heat by convection according to Fig. 9.

4 Conclusion

Based on the thermal-imaging technology, IR camera was used to measure the wall temperature of two kinds of steel tubes with inner diameters of 169 m and 399 m, respectively. Some conclusions from the present experiments are as follow:

1) The local wall temperature distribution on a microtube can by effectively measured by an IR camera.

2) The influence of the axial wall conduction heat on the convective heat transfer is weak as a liquid flows through a steel tube and the axial wall conduction can be neglected compared to the convection.

[References]

[1] Tuckermann D B, Pease R F. Optimized convective cooling using micromachined structure[J]. J Electrochem Soc, 1982, 129(3): C98.

[2] Wu P Y, Little W A. Measurement of friction factor for flow of gases in very fine channels used for microminiature Joule-Thompson refrigerators[J]. Cryogenics, 1983, 24(8): 273-277.

[3] Choi S B, Barren R R, Warrington R O. Fluid flow and heat transfer in micro tubes[J]. ASME DSC, 1991(40): 89-93.

[4] Wang B W, Peng X F. Experimental investigation on forced-flow convection of liquid flow through microchannels[J]. Int J Heat Mass Transfer, 1994, 37(1): 73-82.

[5] Peng X F, Peterson G P. The effect of thermofluid and geometric parameters on convection of liquid through rectangular microchannels[J]. Int J Heat Mass Transfer, 1995, 38(4): 755-758.

[6] Yu D, Warrington R, Barron R, et al. An experimental and theoretical investigation of fluid flow and heat transfer in microtubes[J]. ASME/JSME Thermal Engineering Conference, 1995(1): 523-530.

[7] Adams T M, Abdel-Khalic S I, Jeter S M, et al. An experimental investigation of single-phase forced convection in microchannels[J]. Int J Heat Mass Transfer, 1998, 41(6-7): 851-857.

[8] Ravigururajanm T S, Cuta J, McDonald C E, et al. Single-phase flow thermal performance characteristics of a parallel microchannel heat exchanger[C]// National Heat Transfer Conference, ASME HTD-329, 1996(7): 157-166.

[9] Guo Zengyuan, Li Zhixin. Size effect on microscale single-phase flow and heat transfer, Proceeding of the twelfth International Heat Transfer Conference[C]// Grenoble France, 2002(4): 1058-1069.

[10] Mori S, Sakakibara M, Tanimoto A. Steady heat transfer to laminar flow in a circular tube with conduction in tube wall[J]. Heat Transfer-Jpn Res, 1974, 3(2): 37-46.

[11] Judy J, Maynes D, Webb B W. Characterization of frictional pressure drop for liquid flows through microchannels[J]. Int J Heat and Mass Transfer, 2002, 45(17): 3477-3489.

[12] Weilin Qu, Gh Mohiuddin Mala, Li Dongqing. Heat transfer for water flow in trapezoidal silicon microchannels[J]. Int J Heat and Mass Transfer, 2000, 43(21): 3925-3936.

[责任编辑: 刘 健]